Bulletin of the Earthquake
Research Institute
Vol. 46 (1968), pp. 1001-1025

50. *Deep Structure of Island Arcs as Revealed by Surface Waves.*

By Hiroo Kanamori and Katsuyuki Abe,

Earthquake Research Institute.

(Read Feb. 27, 1968.—Received July 16, 1968.)

Abstract

Group velocities of Rayleigh and Love waves have been measured for a period range 20 to 110 sec to study regional differences in deep island arc structure. Three-component long-period seismographs were used for the measurements. Two horizontal components, NS and EW, were transformed to transverse and radial components to facilitate a separation of Love and Rayleigh waves. Group velocities were determined on both time and frequency domains; band-pass filtering was used on the time domain, and the group delay time $d\phi/d\omega$ (ϕ: phase, ω: angular frequency) was measured on the frequency domain. At the period of 100 sec, the group velocities of Love waves measured for earthquakes near the West Caroline Islands and the Banda Sea are 0.15 km/sec lower than those measured for an earthquake near the Aleutian Islands. A similar trend was found for Rayleigh waves; the velocity difference is 0.15 km/sec at 80 sec. A major portion of the propagation path from the West Caroline Islands and the Banda Sea is above, and on the continental side of, the deep seismic plane, while that from the Aleutian Islands is on the oceanic side. These suggest that the mantle structure is markedly different across the deep seismic plane; the shear velocity is 0.3 to 0.4 km/sec lower over a depth range 30 to 60 km on the continental side than on the oceanic side of the deep seismic plane. No appreciable difference from the normal continental dispersion was found for the path from Eurasia.

Introduction

The regional differences of mantle structures have been revealed by seismic body and surface wave studies. The surface-wave approach is particularly useful for the study of deep structures under oceans where no seismographs can be installed. This paper describes the measurements and the interpretations of group velocities of Rayleigh

and Love waves at island arcs around Japan to a period of 110 sec.

The surface wave studies of the Pacific crust and mantle were summarized by *Ewing et al.* [1962] (see also *Kovach* [1965]). *Oliver et al.* [1955] found an anomalous structure under the Easter Island Rise from the group velocity of Rayleigh waves to the period of 35 sec. Although this period is not long enough to determine detailed deep features, they succeeded in revealing a regional difference in the mantle structure through a careful estimate of the effects of the water layer, sediments, and crustal structures on the dispersion. *Kovach and Press* [1961] found that the group velocity of Rayleigh waves for the path from the Easter Island area to Pasadena is lower than that for normal Pacific paths. They attributed this low group velocity to a relatively low mean shear velocity, 4.5 km/sec, in the upper mantle. A crustal structure derived from refraction studies was incorporated in their interpretation. In these studies, independent knowledge of relatively shallow structures (water, sediment, and crust) played an important role in determining deep structures from relatively short-period waves. *Santo* [1961 *a*, *b*] introduced the "crossing path" technique in order to classify the dispersion character of Rayleigh and Love waves in the Pacific. His classification clearly shows that the dispersion character becomes more continental when the path traverses a part of the region on the continental side of the andesite line. *Saito and Takeuchi* [1965] tested a number of models against Santo's data. Because of the limited period range ($T \leq 40$ sec), however, it was not clear whether the regionality of the dispersion is caused by crustal effects, mantle effects, or both. The results of *Kuo et al.* [1962], who measured phase and group velocities of Rayleigh waves in the Pacific to the period of 140 sec, most strongly suggest that a regional difference may extend down to the mantle. They found that the phase velocities for the Melanesian path to the west of the andesite line are significantly lower, even at long periods, than those for other paths in the Pacific.

In the present study, we tried to extend the period range to as long a period as possible for relatively short paths in order to reveal a difference in deep structures among regions with distinct tectonic features. To sample a region of a distinct tectonic feature, it is necessary to take a relatively short path; if we take a long path, the regional characters will be averaged out. When the path length becomes shorter, however, the detection and the measurement of long-period waves become very difficult. This difficulty is partially removed here by making a cross check

between two independent sets of determination of the group velocity : one in the time domain, and the other in the frequency domain. In the time domain, the band-pass filtering was used whereas in the frequency domain, the group delay time was measured.

Data

Table 1 lists the data of earthquakes studied. The hypocenter data are taken from the Earthquake Data Report (EDR) of the United States Coast and Geodetic Survey (USCGS). Figure 1 shows the propagation paths from the epicenters to Japan. The seismograph system used here consists of the Press-Ewing type pendulum and an amplifier with a RC integrating network whose transfer characteristic is equivalent to a long-period galvanometer (for details, see *Tsujiura* [1965]). The three-component pendulums are installed at Dodaira Micro-Earthquake Observatory (35.998°N,

Table 1. List of Earthquakes.

Region	Date	Origin Time (GMT)	Latitude (deg)	Longitude (deg)	Depth (km)	Magnitude m^a	Magnitude M^b	USCGS EDR[c] No.
Mongolia	Jan. 20, 1967	01 57 23.1	48.0N	102.9E	33R[d]	6.1	6.9	5-67
Aleutian Is.	Jan. 28, 1967	13 52 58.3	52.4N	169.5W	47R	5.9	6.5	8-67
West Caroline Is.	July 20, 1967	15 36 20.1	7.7N	134.9E	8	5.8	6.5	46-67
Turkey	July 22, 1967	16 56 53.3	40.7N	30.8E	4	6.0	7.2	49-67
Banda Sea	Jan. 14, 1968	12 25 09.7	7.5S	127.9E	115R	5.9	6.1	6-68

a Body-wave magnitude as determined by the U. S. Coast and Geodetic Survey.
b Average surface wave magnitude.
c Number of Earthquake Data Reports of the U. S. Coast and Geodetic Survey.
d Restrained depth.

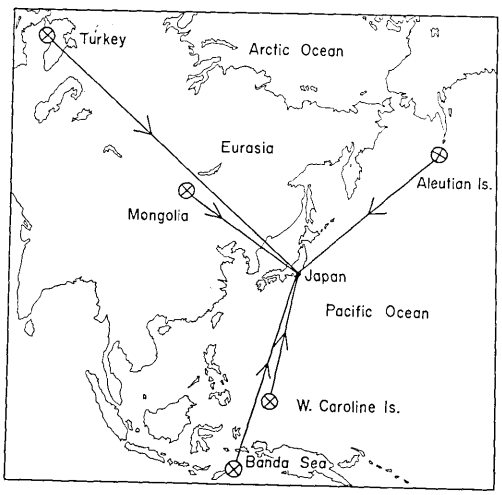

Fig. 1. Epicenters and the great circle paths to Dodaira (DDR) observatory.

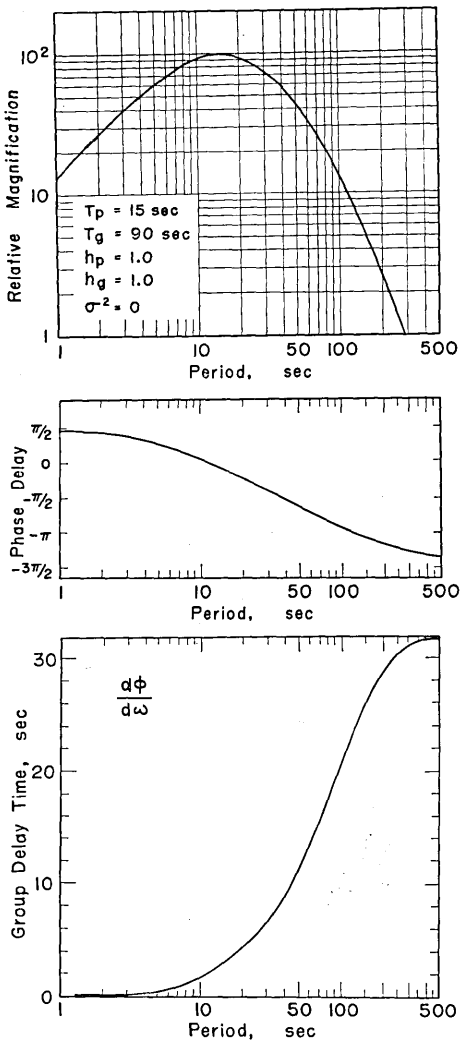

Fig. 2. Instrument constants, relative magnification, phase delay, and group delay of the long-period seismograph used for the analysis. The constants T_p and h_p are natural period and damping constant of the pendulum, and σ is the coupling factor as given by *Hagiwara* [1958]. The constants T_g and h_g are natural period and damping constant of the equivalent galvanometer.

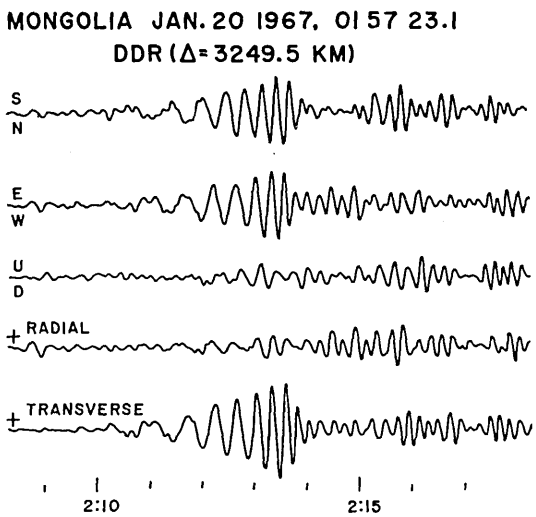

Fig. 3. Five-component (S-N, E-W, U-D, radial, and transverse) seismogram reproduced from a digital output for the Mongolia earthquake recorded at Dodaira. The signs are taken positive for the motions away from the epicenter (radial), and counterclockwise around the epicenter as seen from above (transverse).

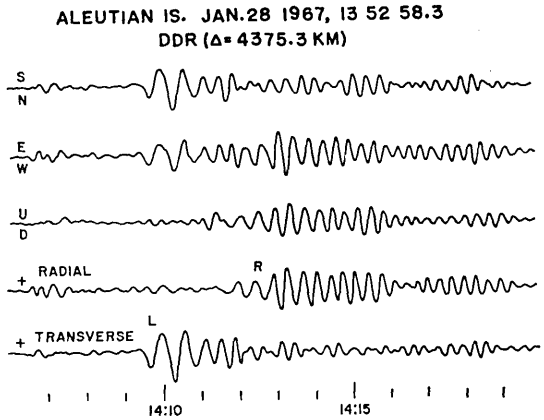

Fig. 4. Five-component (S-N, E-W, U-D, radial, and transverse) seismogram reproduced from a digital output for the Aleutian Is. earthquake recorded at Dodaira.

139.193°E, height 0.8 km). The equivalent instrument constants and the characteristic curves calculated by *Hagiwara's* [1958] formula are given in Fig. 2. The frequency-modulated signal is microwave-telemetered from the station to the Earthquake Research Institute, where it is recorded on magnetic tapes, discriminated, and digitized at a 1 sec interval. In order to facilitate the distinction between modes with radial and transverse motions, horizontal components were decomposed into radial and transverse directions, and synthesized. The advantage of this procedure has been described by *Press* [1966, p. 249]. The sign of the radial component is taken positive when the motion is away from the epicenter; for the transverse component, it is taken positive when the motion is counterclockwise around the epicenter (seen from above). Two examples of the rotated seismograms are shown in Figs. 3 and 4.

Analysis

For the measurement of group velocities we used two methods: (1) Band-pass filtering, and (2) Group-delay time method.

(1) Band-pass filtering method

For a single mode, the seismogram at a distance r from an epicenter can be written

$$f(t, r)=\int_0^\infty F(\omega, r)\cos[kr-\omega t+\phi_0(\omega)+\phi_I(\omega)]d\omega \qquad (1)$$

(t=time, ω=angular frequency, k=wave number). Here $F(\omega, r)$ includes the amplitude spectrums of the source, the wave guide, and the instrument. The functions $\phi_0(\omega)$ and $\phi_I(\omega)$ are the phase delays at the source and that due to the instrument respectively. The band-pass filtered seismogram centered at $\omega=\omega_i$ and of width $\Delta\omega_i$ is

$$\tilde{f}(t, r)=\int_{\omega_i-\Delta\omega_i/2}^{\omega_i+\Delta\omega_i/2} F(\omega, r)\cos[kr-\omega t+\phi_0(\omega)+\phi_I(\omega)]d\omega$$

$$\sim\Delta\omega_i F(\omega_i, r)\cos(k_i r-\omega_i t+\phi_{0,i}+\phi_{I,i})\frac{\sin\left\{[k_i' r-(t-\phi_{0,i}'-\phi_{I,i}')]\dfrac{\Delta\omega_i}{2}\right\}}{\left\{[k_i' r-(t-\phi_{0,i}'-\phi_{I,i}')]\dfrac{\Delta\omega_i}{2}\right\}} \qquad (2)$$

where the subscript i refers to the value at $\omega=\omega_i$, and the prime

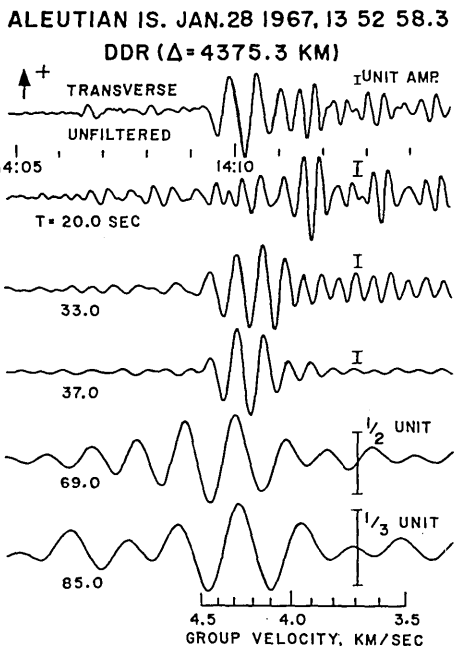

Fig. 5. Band-pass filtered seismograms of the transverse component of the Aleutian Is. earthquake. Love wave trains are shown. The vertical bar indicates the unit of the relative amplitude scale. The predominant periods are given by T. The group velocity scale is not corrected for the instrument delay.

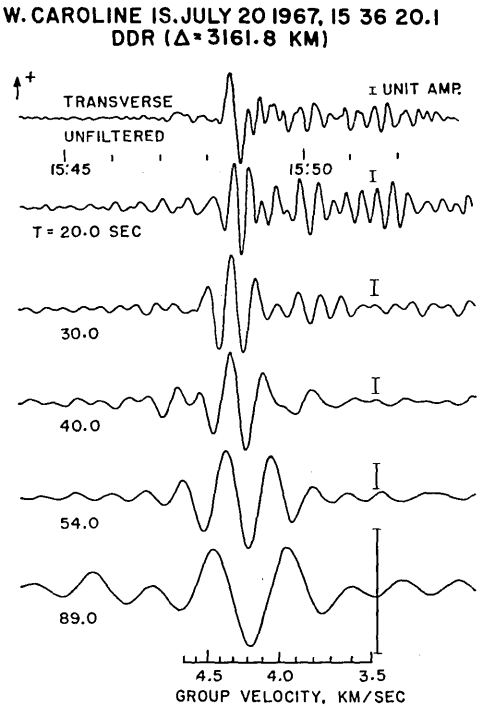

Fig. 6. Band-pass filtered seismograms of the transverse component of the West Caroline Is. earthquake. Love wave trains are shown.

indicates the derivative with respect to ω. The quantities $(k_i')^{-1}$, $\phi_{0,i}'$ and $\phi_{I,i}'$ are the group velocity, the group delay time at the source, and the group delay time due to the instrument respectively. In the above, it is assumed that

$$\left|\frac{\Delta\omega_i}{F_i}F_i'\right| \ll 1, \qquad \left|\frac{(\Delta\omega_i)^2}{k_i}k_i''\right| \ll 1, \qquad \left|\frac{(\Delta\omega_i)^2}{\phi_{0,i}}\phi_{0,i}''\right| \ll 1,$$

and

$$\left|\frac{(\Delta\omega_i)^2}{\phi_{I,i}}\phi_{I,i}''\right| \ll 1, \tag{3}$$

The band-pass filtered seismogram $\bar{f}(t, r)$ is a wave train whose envelope

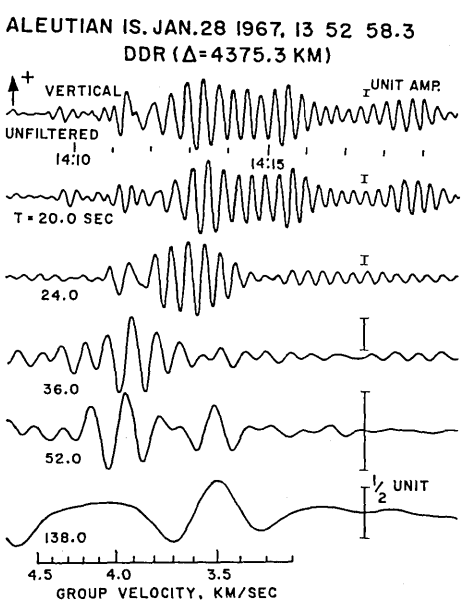

Fig. 7. Band-pass filtered seismograms of the vertical component of the Aleutian Is. earthquake. Rayleigh wave trains are shown. The trace with $T=138.0$ sec was not used for the interpretation.

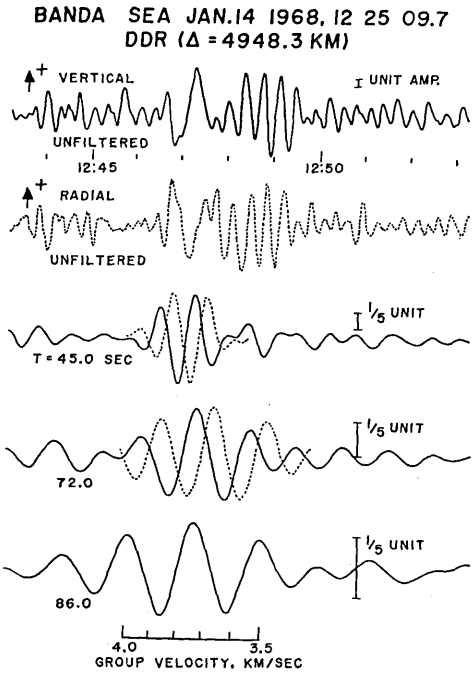

Fig. 8. Band-pass filtered seismograms of the vertical component of the Banda Sea earthquake. Rayleigh wave trains are shown. Radial components (dotted curve) are superposed on the vertical component. The amplitude of the radial components is arbitrary.

takes a maximum at $t_M=k_i'r+\phi_{0,i}'+\phi_{I,i}'$, and whose effective length is $2\pi/\Delta\omega_i$. The bandwidth $\Delta\omega_i$ has to be chosen large enough to make $2\pi/\Delta\omega_i$ sufficiently short, yet $\Delta\omega_i$ should be small enough to satisfy the conditions given by (3). By determining t_M on the band-pass filtered seismogram, we can determine the group velocity:

$$U_i\equiv(k_i')^{-1}=\frac{r}{t_M-\phi_{0,i}'-\phi_{I,i}'}\,. \tag{4}$$

The instrumental group delay $\phi_{I,i}'$ can be calculated from the instrumental constants and is plotted in Fig. 2. The source group delay time $\phi_{0,i}'$ depends on the source time function. When the source time function is an impulse or a step function, $\phi_{0,i}'$ vanishes. For a ramp function

with a build-up time of τ_0, $\phi'_{0,i}$ is equal to $\tau_0/2$. In general, $\phi'_{0,i}$ is of the order of half the duration time of the major motion at the source. Because the magnitude of the earthquakes used here is about 6 to 7, the associated fault length is probably about 20 km [*Tocher*, 1958; *Iida*, 1965], and, with a rupture velocity of 4 km/sec, the duration time is 5 sec. Thus the source group delay $\phi'_{0,i}$ is about 3 sec and is less than 0.5% of the total travel time, about 700 sec. We therefore ignored $\phi'_{0,i}$ in the present analysis.

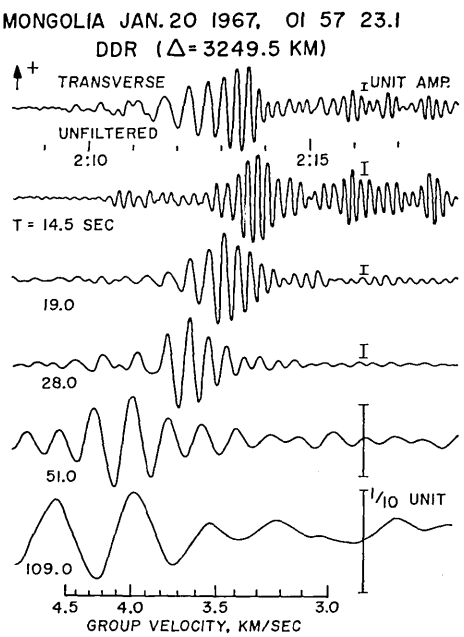

Fig. 9. Band-pass filtered seismograms of the transverse component of the Mongolia earthquake. Love wave trains are shown. The trace with $T=$ 109.0 sec was not used for the interpretation.

We analyzed a seismogram of 1024 sec length which includes the surface wave train near the center. The data were not tapered. We took 512 digitized points with a 2 sec interval. With this interval, no serious aliasing is caused. We first Fourier analyzed the data, selected the harmonic components to be passed, and then synthesized these components to produce the band-pass filtered seismogram. These analyses were greatly facilitated by the method developed by *Cooley and Tukey* [1965]. Several examples of the band-pass filtered seismogram are shown in Figs. 5, 6, 7, 8, and 9. It was recognized that the band-pass filtering made on a digital seismogram is very useful in detecting weak long-period waves.

(2) Group-delay time method

From equation 1, the phase of a component wave at a distance r, and at a time t_0 is

$$\phi(t_0, \omega) = kr - \omega t_0 + \phi_0(\omega) + \phi_I(\omega) \ . \qquad (5)$$

Taking the derivative with respect to ω, we can write the group velocity $U(\omega) \equiv \partial\omega/\partial k$ as

$$U(\omega)=\frac{r}{t_0+\dfrac{\partial\phi(t_0,\omega)}{\partial\omega}-\dfrac{d\phi_0(\omega)}{d\omega}-\dfrac{d\phi_I(\omega)}{d\omega}}\ .$$

The quantity $t_0+\partial\phi(t_0,\omega)/\partial\omega$ is called the group delay time [*Aki*, 1960]. By "group delay" is meant the following. The phase at an arbitrary time t can be written as

$$\phi(t,\omega)=\phi(t_0,\omega)+\omega(t_0-t)\ . \tag{6}$$

Similarly, for an angular frequency $\omega+\delta\omega$,

$$\phi(t,\omega+\delta\omega)=\phi(t_0,\omega)+(\omega+\delta\omega)(t_0-t)\ . \tag{7}$$

Suppose that at a time $t=t_g$, $\phi(t,\omega)$ equals $\phi(t,\omega+\delta\omega)$. At this time, the component wave with angular frequency ω interferes constructively with that with $\omega+\delta\omega$ to yield a maximum of energy. This time may most naturally be called the group delay time. By equating (6) to (7), we can derive

$$t_g=t_0+\frac{\partial\phi(t_0,\omega)}{\partial\omega}$$

($\partial\phi(t_0,\omega)/\partial\omega$ may be called the group delay time measured from t_0).

The experimental group delay times were determined by the conventional Fourier technique from digitized seismograms of 512 sec length (1 sec interval), which include the major portion of either Rayleigh or Love waves to be studied. The data were detrended and tapered at both ends; the length of the tapered portion ranges from 20 to 50% of the total length depending upon the nature of the seismogram. Fig. 10 compares the group velocities thus calculated from the group delay times with those determined by the band-pass filtering. In these examples, no appreciable difference is seen between the results from the two sets of data. While analysing the data, however, we realized that the band-pass filtering is more useful than the group-delay time method when the seismogram is contaminated by body waves or higher mode surface waves. The group delay times, on the other hand, give a more accurate and objective estimate of the group velocity when the noise is absent. We determined most of the group velocities by the band-pass filtering while referring to, and cross-checking with, the group delay times.

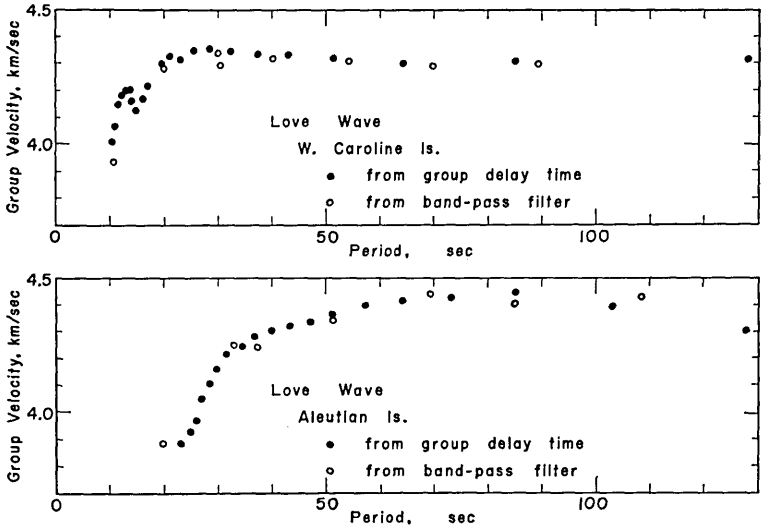

Fig. 10. Comparison of group velocities determined by the band-pass filtering and the group delay time method.

Results and Interpretation

Oceanic Love waves

Figure 11 shows the group velocities of Love waves for three oceanic paths. The average water depths are 3.6, 3.7, and 2.9 km for the Aleutian Is., W. Caroline Is., and Banda Sea paths respectively. At periods shorter than 50 sec, the observed group velocities show a complicated variation with period. The gradual fall-off towards shorter periods for the Aleutian path presumably reflects the fact that a part of the path grazes the Aleutian Islands; a thicker crust beneath the islands must have delayed short-period waves. The same applies to the Banda Sea path which traverses the East Indies. At longer periods, however, a distinct difference is exhibited

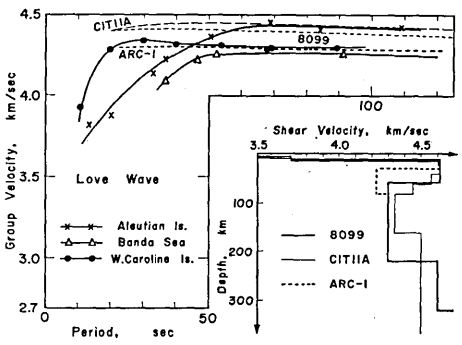

Fig. 11. Group velocities of oceanic Love waves as compared with those for three models. The shear velocity distributions for the three models are given.

Table 2. ARC-1 model.

Layer Number	Layer Thickness	Shear Velocity
1	5 km	0.0 km/sec
2	1	1.0
3	5	3.7
4	19	4.6125
5	50	4.23

Note: The distribution of S velocity below 80 km is identical to that of the 8099 model (see Appendix). The distributions of P velocity and density are identical to those of the 8099 model. The effect of P velocity on the group velocity is small; a change of 0.35 km/sec in P velocity over a depth range from 10 to 60 km causes a change of about 0.02 km/sec in group velocity of Rayleigh waves for the period range considered.

Table 3. Order number N, period T, phase velocity C, and group velocity U for the ARC-1 model.

N	Rayleigh Wave			Love Wave		
	T (sec)	C (km/sec)	U (km/sec)	T (sec)	C (km/sec)	U (km/sec)
250	40.8	3.913	3.774	36.4	4.390	4.303
200	50.6	3.948	3.793	45.2	4.411	4.301
150	66.6	3.995	3.797	59.7	4.449	4.296
120	82.1	4.046	3.778	74.0	4.487	4.292
100	97.0	4.105	3.746	87.9	4.526	4.289
80	118.6	4.192	3.714	108.4	4.586	4.285

between the group velocities for the Aleutian path and the other two paths (Banda Sea and West Caroline Islands paths). The group velocity at 100-sec period is 4.45 km/sec for the former whereas it is 4.30 km/sec for the latter paths.

It is not meaningful to fit short period group velocity curves measured over a horizontally heterogeneous path by a group velocity curve calculated for a horizontally homogeneous model. Hence, we considered only long period portions of the data and tried to interpret them in terms of a broad structure of the upper mantle. The group velocity at a 100-sec period is not greatly affected by shallower structures, but is mainly governed by the upper mantle structure. Although the group velocity method is not so straightforward as the phase velocity

method, we believe that the group velocity at 100 sec is useful for delineating a gross features of the upper mantle.

In Fig. 11, the dispersion curves for two existing oceanic models, 8099 [*Dorman et al.* 1960] and CIT 11 A [*Anderson and Toksöz*, 1963; *Kovach*, 1965; see also *Anderson*, 1967] are included (see also Appendix). The group velocities for the Aleutian path fall around the curve for CIT 11 A model at $T>60$ sec. The CIT 11 A model has a slightly higher velocity in the top 100 km of the mantle as compared with the 8099 model. The group velocities for the Banda Sea, and the West Caroline paths are definitely lower than that for the Aleutian path at $T>60$ sec. This difference amounting to 0.15 km/sec at $T\sim100$ sec cannot be explained in terms of shallower structures alone. A gross difference in the upper mantle structure has to be invoked. A number of models were tried to fit the group velocities for the Banda Sea and the West Caroline paths. A model designated as ARC-1 (see Fig. 11, Tables 2 and 3) emerges from these trials; it fits the observed group velocities reasonably well over the period range 50 to 120 sec. Because of the limited period range ($T<120$ sec), little can be said about the mantle below 150 km. The major difference of the ARC-1 model from the normal oceanic model lies in the depth range 30 to 60 km; over this depth range, the S velocity is lower by 0.38 km/sec for the ARC-1 model than for the normal oceanic model.

Oceanic Rayleigh waves

Figure 12 shows the group velocities of Rayleigh waves for two oceanic paths. The group velocities at 80-sec period are 3.95 and 3.80 km/sec for the Aleutian and the Banda Sea paths respectively. No Rayleigh waves with an appreciable amplitude were observed for the earthquake from the West Caroline Islands. The group velocity curve for the CIT 11 A model fits the data for the Aleutian path reasonably well, and the curve for the ARC-1 model fits the data for the Banda Sea path. Thus, the CIT 11 A and ARC-1 models can explain both Rayleigh and Love wave dispersions for the Aleutian and

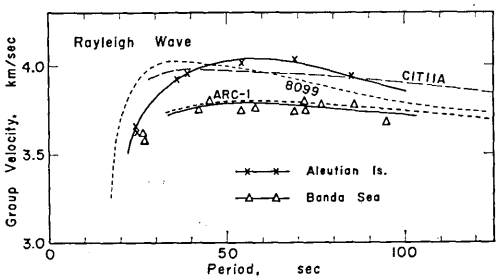

Fig. 12. Group velocities of oceanic Rayleigh waves. The shear velocity distributions for the three models are given in Fig. 11.

the Banda Sea paths respectively. It is to be noted that ARC-1 model also explains well the phase and group velocity data for the Melanesia-New Zealand region reported by *Kuo et al.* [1962].

Discussions for the Oceanic Paths

So far, a striking contrast of the dispersion character has been shown to exist between the Aleutian path and the two paths from the south (Banda Sea path, and the West Caroline Is. path). These paths are also characterized by distinct tectonic features. Figure 13 shows the location of these paths with respect to the deep seismic zone, trench, and the volcanic front. The volcanic front defined by *Sugimura* [1960], is the boundary where volcanoes suddenly become sparse towards the ocean. The volcanic front roughly coincides with the location of volcanic ridges.

A major portion of the path from the Aleutian Islands lies on the oceanic side of the deep seismic plane, volcanic ridge, and trench (see also Fig. 14). A cross section normal to the path is taken at A in Fig. 13, and is shown in Fig. 15. Open circles are earthquake foci deeper than 60 km determined by USCGS for the interval January 1963 to June 1966. In contrast, the paths from the south lie above the seismic plane, and on the continental side of the volcanic ridge and the trench (Figs. 13 and 14). This situation is visualized in Fig. 16 which shows a cross section normal to the path taken at B in Fig. 13. It may now be concluded that a distinct difference exists between the mantles separated by the deep seismic plane; the S velocity is lower by 0.3 to 0.4 km/sec over the depth range 30 to 60 km on the continental side than on the oceanic side of the deep seismic plane. The boundary also coincides with the location of other major tectonic features such as volcanic ridge and trench.

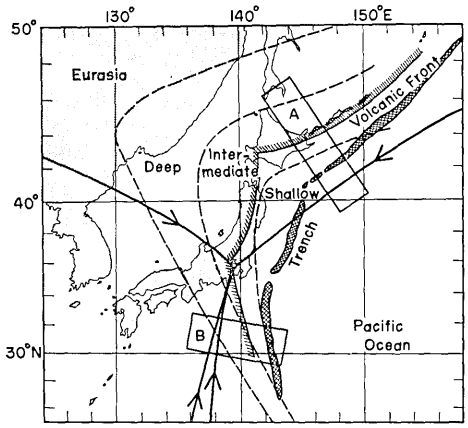

Fig. 13. The location of seismic zones (deep, intermediate, and shallow), trench, and volcanic front with respect to the great circle paths. The cross sections are taken at A and B and are shown in Figs. 15 and 16.

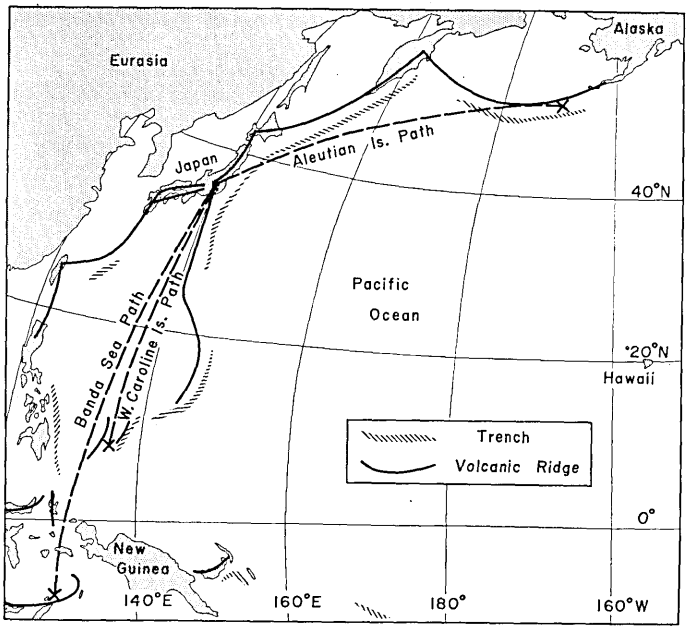

Fig. 14. Great circle paths from the Aleutian Is., West Caroline Is., and Banda Sea with respect to trench and volcanic ridge. Note that the entire path from the Aleutian Is. is on the oceanic side of the volcanic ridge, and those from the West Caroline Is. and Banda Sea are on the continental side of the volcanic ridge.

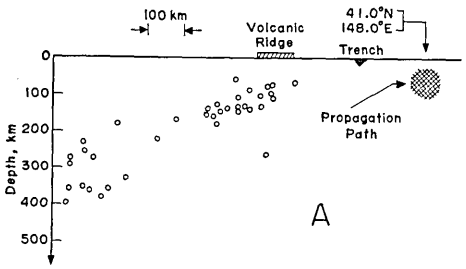

Fig. 15. A cross section taken at A in Fig. 13.

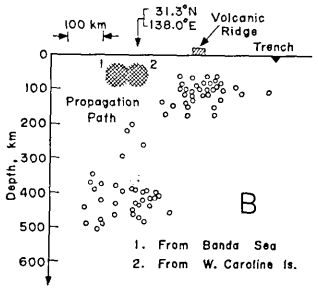

Fig. 16. A cross section taken at B in Fig. 13.

The earthquake foci (open circle) are taken from EDR of USCGS for Jan. 1963 to June 1966 ($d \geq 60$ km). The scatter is partly due to the obliquity of the seismic plane with respect to the cross section considered. The crosshatched part indicates an approximate area sampled by the surface waves.

Continental Love and Rayleigh Waves

The group velocities of Love waves measured for the earthquakes in Turkey and Mongolia are shown in Fig. 17. The group velocities of Rayleigh waves were measured only for the earthquake in Turkey (Fig. 18). In Figs. 17 and 18, theoretical curves for the Gutenberg model (see Appendix), and the experimental curves by *Porkka* [1966], and after *Kovach* [1965] are included.

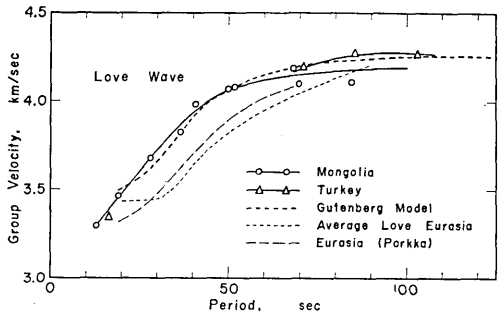

Fig. 17. Love wave group velocities for the continental paths. The average for Eurasia is taken from *Kovach* [1965].

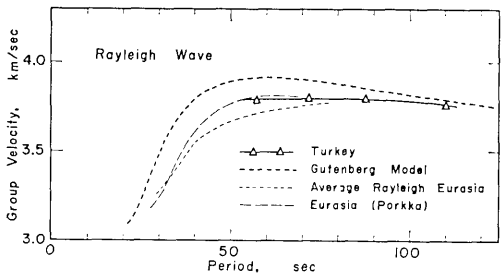

Fig. 18. Rayleigh wave group velocities for the continental path. The average for Eurasia is taken from *Kovach* [1965].

The path from Mongolia consists 75% of continent with an average elevation of 0.9 km, and 25% of ocean (Japan Sea) with an average depth of 2.5 km. The path from Turkey consists 85% of continent with an average height of 0.5 km and 15% ocean with an average water depth of 2.5 km. These paths are thus predominantly continental, but it is still difficult to interpret the short-period group velocities in terms of a homogeneous model. We only note here that the group velocities for both Rayleigh and Love waves tend to agree with the average curves for Eurasia given by Porkka and Kovach towards long periods.

Uniqueness and Accuracy

The effect of shallow structures

In the interpretation of the oceanic dispersions we only modified the mantle structure, ignoring the effect of structures such as water layer, sedimentary layer, and the crust. In view of the non-unique-

ness of the group velocity method, we made a numerical check to see the effect of shallow structures on the group velocity. Starting from the 8099 model we constructed three models, S, C, and M models (Fig. 19). The S model is so designed that we can see the effect of water and sedimentary layer. The water layer 1 km thick is substituted by a sedimentary layer. The effect of this modification is very small for both Love and Rayleigh waves as shown in Fig. 19. To see the effect of crustal thickening, the C model is constructed. The crust of the 8099 model is thickened from 5 to 14 km. The effect on the Rayleigh and Love wave group velocities are about 0.03 and 0.06 km/sec respectively at long periods. We see that these values are relatively small even for such an extensive thickening as that incorporated in model C. It is improbable that the actual crustal thickening, on the average, exceeds 5 km. We therefore ignore the crustal effect and conclude that the observed low group velocity is the manifestation of the mantle effect. The effect of the mantle is demonstrated by the M model (Fig. 19) which we constructed from the 8099 model by removing the high velocity lid extending from 11 to 60 km depth. As Fig. 19 shows, the effects are of the right order of magnitude for explaining the observed low velocities. It is to be noted, however, that whether the high velocity lid should be totally or partially removed cannot be decided with the group velocity data alone. In constructing the ARC-1 model, we incorporated the results of refraction studies by *Murauchi et al.* [1968] who reported that the basins of the

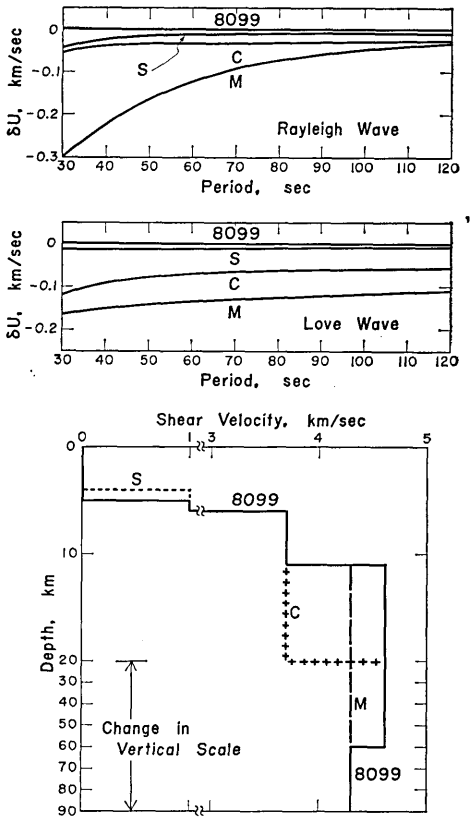

Fig. 19. The effect of sediment, crust, and mantle structure on the group velocity of Love and Rayleigh waves. The 8099 model is taken as a standard. The deviations of the group velocity from that of the 8099 model are shown for three models, S, C, and M.

Philippine Sea have a normal oceanic crust and normal P_n velocities. We therefore removed only the lower part of the high velocity lid keeping the velocity just below the Moho discontinuity unchanged.

Source of error

The largest error arises from the contamination of the seismogram by instrumental noise, multiply reflected body phases, and higher mode surface waves. These noises are usually difficult to eliminate except by the eyesight judgment of the interpreter. The band-pass filtering used here greatly facilitates the eyesight removal of the noise. For example, the band-pass filtered seismogram of the Aleutian earthquake (Fig. 7) shows apparently coherent wave trains with a group velocity of about 3.5 km/sec at $T=52$ and 138 sec. However, from the general appearance of the seismograms we regarded them as spurious, and discarded them. Although this kind of judgment is in no way objective, we believe that the judgments can be correctly made up to a period of about 100 sec. Once the noise has been removed, the numerical measurement of the group velocity is accurate because we used the band-pass filtering and the group delay time method instead of the conventional peak-and-trough method.

Since we intentionally used relatively short paths, the errors in epicenter location can be serious. We referred to the EDR of the U. S. Coast and Geodetic Survey to examine a possible location error. We found rather unsatisfactory station residuals implying a poor hypocenter location for the Banda Sea earthquake. We therefore redetermined the hypocenter using a computer program developed here and the raw data available in the EDR. Since the data are the same as those used by USCGS, no gross improvement is expected. However, we tried to see general uncertainty of the location by redetermining the hypocenter with various restraints and with different selections of the data. The uncertainties of the epicenter distance and the origin time were found to be about 10 km and 5 sec respectively; the resulting error in the group velocity was estimated as ± 0.02 km/sec. This is much smaller than the observed regional difference.

Discussions

The present results call for an extensive lateral variability of the upper mantle structure. A variability of this magnitude is not unwar-

ranted in view of numerous evidence heretofore found. The anomalously low group velocities of Rayleigh waves in the Melanesian-New Zealand region found by *Kuo et al.* [1962] are very close to what we found for the Banda Sea to Japan path. Recent studies at mid-oceanic ridges [see *e.g. Talwani et al.* 1965] and island arcs [*Katsumata*, 1960; *Utsu*, 1966; *Oliver and Isacks*, 1967] all suggest that a large horizontal heterogeneity does exist in the upper mantle. The present results require that the upper mantle velocity beneath the Mariana and Japanese Islands be relatively low as compared with the world average. This has been borne out by *Aki* [1961] who used surface waves, *Fedotov and Slavina* [1968] who used body waves and *Kanamori* [1968] who used the LONGSHOT data. *Fedotov and Slavina* [1968] found a relatively low mantle velocity, 7.5 km/sec, beneath Kamchatka. *Utsu* [1967] and *Kanamori* [1968] have proposed a model in which P velocity in the top 200 to 250 km of the mantle beneath Japan is 0.3 to 0.5 km/sec lower on the continental side than on the oceanic side of the deep seismic plane. Although the depth range concerned is different, these results are compatible with those found by the present study.

Press [1968 *a*, *b*] attempted a Monte Carlo inversion of gross geophysical data and showed that earth models with large fluctuations in shear velocity and density in the upper mantle fit the data better than smooth standard models. He suggested a possibility that the mantle is laterally variable ranging from a pyrolitic to eclogitic composition. These, all in all, suggest that the lateral heterogeneity is larger, both in space and magnitude, than has heretofore been appreciated.

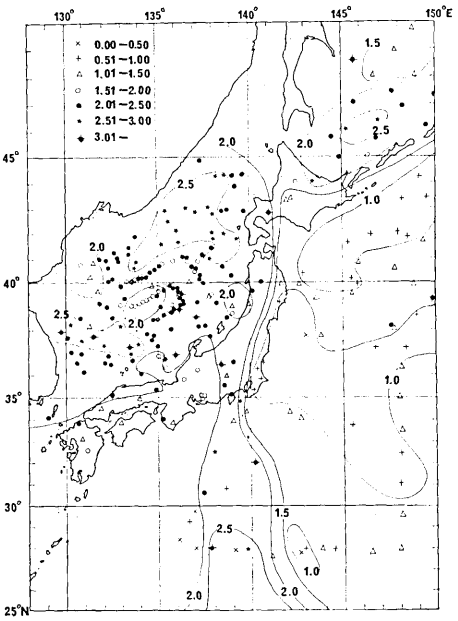

Fig. 20. Heat flow distribution around Japan (after *Vacquier et al.* [1966]). The unit is μcal/cm^2 sec.

A remarkable correlation exists between the group velocity and heat flow. Figure 20 shows a map of heat flow distribution around Japan given by *Vacquier et al.* [1966]. The path from the Aleutian Islands for

which the group velocity is relatively high traverses a low heat flow region, while the path from the south for which the group velocity is low traverses a region of extremely high heat flow. This correlation implies common causes, namely, a temperature effect, and presumably a partial fusion. The partial fusion reduces the strength of the mantle and decouples the crust from the mantle. Thus, the coincidence of the region underlain by the low velocity mantle with the region of active volcanism, seismicity and crustal movement seems natural, if we adopt the current view that the crust-mantle decoupling is responsible for various tectonic processes [*e.g. Press*, 1959].

Conclusions

The group velocities of Love and Rayleigh waves are measured by the band-pass filtering and the group delay time method. Several paths to Japan crossing regions of distinct tectonic features are studied. These paths are: A. From the Aleutian Islands to Japan, a major portion of which lies on the oceanic side of such tectonic features as deep seismic plane, trench, and volcanic ridge. B. From the West Caroline Islands and Banda Sea to Japan. This path lies almost entirely above the deep seismic plane, and on the continental side of the trench and of the volcanic ridge. C. From Eurasia to Japan intervened, for a small distance, by the Japan Sea. The results are: (1) The long-period group velocities of Love and Rayleigh waves for the path A are about equal to, or slightly larger than, those for the standard oceanic models such as the 8099 and the CIT 11 A models. (2) For the path B, the group velocities at the period of 100 sec are lower by 0.1 to 0.2 km/sec than those for the standard models. These low group velocities can most reasonably be explained if we reduce the mantle shear velocity by 0.3 to 0.4 km/sec over the depth range from 30 to 60 km. This reduction of the velocity is the major feature of the proposed model ARC-1. (3) The dispersion of Love and Rayleigh waves for the path C exhibits no appreciable difference from the average for Eurasia. (4) The regions with high and low group velocities correspond to those with low and high heat flows respectively.

Appendix

The phase and group velocity data for five standard models are presented in the following tables. The models are taken from *Alterman et al.* [1961] (Gutenberg model), *Dorman et al.* [1960] (Jeffreys and 8099 model), *Brune and Dorman* [1963] (CANSD model), and *Kovach* [1965] (CIT 11 A model). A minor modification has been made where necessary.

For the calculation, we wrote a computer program which calculates free periods of a spherically symmetric sphere. We referred to *Alterman et al.* [1959], *Bolt and Dorman* [1961], and *Takeuchi et al.* [1962]. The variational method was used for the calculation of group velocities. The effect of gravity is included for periods longer than 70 sec. The numerical accuracy was checked against the results by *Satô et al.* [1960], *Alterman et al.* [1961], *Bolt and Dorman* [1961], and *Takeuchi et al.* [1964]. Our results agree to at least three significant digits with the published results.

JEFFREYS-BULLEN A

N	THICKNESS KM	ALPHA KM/SEC	BETA KM/SEC	RHO G/CC
1	15.0	5.5700	3.3600	2.6500
2	18.0	6.5000	3.7400	2.8700
3	17.0	7.7750	4.3600	3.3300
4	25.0	7.8300	4.3900	3.3500
5	35.0	7.9200	4.4400	3.3700
6	40.0	8.0400	4.4900	3.4100
7	50.0	8.1900	4.5600	3.4500
8	50.0	8.3500	4.6400	3.4900
9	50.0	8.5000	4.7200	3.5300
10	50.0	8.6700	4.8000	3.5700
11	63.0	8.8600	4.9000	3.6150
12	37.0	9.1400	5.0400	3.7000
13	100.0	9.6500	5.3100	3.8900
14	100.0	10.2500	5.6600	4.1250
15	100.0	10.6800	5.9300	4.3200
16	100.0	11.0000	6.1300	4.4900
17	150.0	11.2800	6.2900	4.6200
18	200.0	11.5700	6.4400	4.7390
19	400.0	11.9900	6.6200	4.9150
20	400.0	12.5300	6.8300	5.1350
21	400.0	13.0300	7.0200	5.3400
22	400.0	13.5000	7.2100	5.5400
23	98.0	13.6400	7.3000	5.6900

RAYLEIGH WAVE

N	T SEC	C KM/SEC	U KM/SEC
25	294.9	5.323	3.907
30	258.7	5.073	3.776
40	208.7	4.736	3.725
50	174.8	4.534	3.752
60	150.2	4.405	3.787
80	116.9	4.253	3.822
100	95.7	4.164	3.824
120	81.0	4.104	3.81
150	65.7	4.046	3.77
200	50.3	3.969	3.72
250	40.9	3.908	3.61
300	34.6	3.850	3.50
350	30.1	3.791	3.39

LOVE WAVE

N	T SEC	C KM/SEC	U KM/SEC
25	296.3	5.299	4.429
30	254.8	5.152	4.384
35	223.7	5.042	4.357
40	199.4	4.956	4.337
50	164.1	4.830	4.308
55	150.8	4.783	4.294
60	139.5	4.742	4.281
65	129.9	4.706	4.268
71	119.9	4.669	4.251
80	107.6	4.620	4.226
86	100.8	4.592	4.208
100	87.8	4.536	4.167
120	74.3	4.470	4.11
150	60.6	4.388	4.02
200	46.7	4.277	3.87
250	38.2	4.181	3.73
300	32.5	4.096	3.62
350	28.4	4.021	3.53

GUTENBERG-BULLEN A

N	THICKNESS KM	ALPHA KM/SEC	BETA KM/SEC	RHO G/CC
1	19.0	6.1400	3.5500	2.7400
2	19.0	6.5800	3.8000	3.0000
3	12.0	8.2000	4.6500	3.3200
4	10.0	8.1700	4.6200	3.3400
5	10.0	8.1400	4.5700	3.3500
6	10.0	8.1000	4.5100	3.3600
7	10.0	8.0700	4.4600	3.3700
8	10.0	8.0200	4.4100	3.3800
9	25.0	7.9300	4.3700	3.3900
10	25.0	7.8500	4.3500	3.4100
11	25.0	7.8900	4.3600	3.4300
12	25.0	7.9800	4.3800	3.4600
13	25.0	8.1000	4.4200	3.4800
14	25.0	8.2100	4.4600	3.5000
15	50.0	8.3800	4.5400	3.5300
16	50.0	8.6200	4.6800	3.5800
17	50.0	8.8700	4.8500	3.6200
18	50.0	9.1500	5.0400	3.6900
19	50.0	9.4500	5.2100	3.8200
20	100.0	9.8800	5.4500	4.0100
21	100.0	10.3000	5.7600	4.2100
22	100.0	10.7100	6.0300	4.4000
23	100.0	11.1000	6.2300	4.5600
24	100.0	11.3500	6.3200	4.6300
25	200.0	11.6000	6.4200	4.7400
26	200.0	11.9300	6.5500	4.8500
27	200.0	12.1700	6.6900	4.9600
28	200.0	12.4300	6.8000	5.0700
29	200.0	12.6700	6.9000	5.1900
30	200.0	12.9000	6.9700	5.2900
31	200.0	13.1000	7.0500	5.3900
32	200.0	13.3200	7.1500	5.4900
33	200.0	13.5900	7.2300	5.5900
34	98.0	13.7000	7.2000	5.6900

RAYLEIGH WAVE

N	T SEC	C KM/SEC	U KM/SEC
25	296.4	5.296	3.824
30	260.6	5.036	3.664
40	211.2	4.681	3.585
50	177.5	4.465	3.617
60	152.9	4.328	3.673
80	119.1	4.176	3.769
100	97.1	4.101	3.838
120	81.8	4.060	3.88
150	66.0	4.032	3.91
200	49.9	4.001	3.90
250	40.2	3.971	3.79
300	33.9	3.928	3.64
350	29.5	3.873	3.45

LOVE WAVE

N	T SEC	C KM/SEC	U KM/SEC
25	300.5	5.224	4.348
30	258.5	5.077	4.312
35	227.0	4.968	4.295
40	202.4	4.884	4.285
50	166.4	4.765	4.277
55	152.8	4.721	4.274
60	141.3	4.684	4.271
65	131.4	4.652	4.268
71	121.2	4.620	4.265
80	108.6	4.580	4.258
86	101.6	4.557	4.252
100	88.2	4.514	4.237
120	74.4	4.465	4.21
150	60.3	4.408	4.15
200	46.1	4.327	4.01
250	37.6	4.247	3.85
300	32.0	4.169	3.72
350	27.9	4.097	3.62

CANSD

N	THICKNESS KM	ALPHA KM/SEC	BETA KM/SEC	RHO G/CC
1	6.0	5.6400	3.4700	2.7000
2	10.5	6.1500	3.6400	2.8000
3	18.7	6.6000	3.8500	2.8500
4	80.0	8.1000	4.7200	3.3000
5	100.0	8.2000	4.5400	3.4400
6	100.0	8.3000	4.5100	3.5300
7	80.0	8.7000	4.7600	3.6000
8	105.8	9.3000	5.1200	3.7600
9	100.0	9.9700	5.4925	4.0100
10	100.0	10.4800	5.7900	4.2300
11	100.0	10.8500	6.0300	4.4100
12	100.0	11.1200	6.2000	4.5450
13	100.0	11.3300	6.3150	4.6400
14	100.0	11.4900	6.4000	4.7100
15	100.0	11.6400	6.4650	4.7700
16	100.0	11.7800	6.5310	4.8275
17	100.0	11.9200	6.5910	4.8825
18	100.0	12.0600	6.6490	4.9400
19	100.0	12.1900	6.7040	5.0000
20	100.0	12.3300	6.7550	5.0550
21	100.0	12.4600	6.8050	5.1050
22	100.0	12.5900	6.8525	5.1575
23	100.0	12.7200	6.8975	5.2075
24	100.0	12.8500	6.9450	5.2650
25	100.0	12.9700	6.9950	5.3150
26	100.0	13.0900	7.0450	5.3650
27	100.0	13.2100	7.0950	5.4150
28	100.0	13.3300	7.1425	5.4650
29	100.0	13.4600	7.1875	5.5150
30	100.0	13.5300	7.2325	5.5625
31	100.0	13.6100	7.2775	5.6075
32	97.0	13.6400	7.3000	5.6550

RAYLEIGH WAVE

N	T SEC	C KM/SEC	U KM/SEC
30	259.2	5.064	3.710
40	209.5	4.718	3.672
50	175.5	4.516	3.746
60	150.6	4.394	3.834
80	116.4	4.270	3.968
100	94.5	4.216	4.042
120	79.2	4.195	4.07
150	63.8	4.170	4.07
200	48.3	4.133	3.98
250	39.2	4.075	3.90
300	33.1	4.027	3.62
350	28.9	3.952	3.47

LOVE WAVE

N	T SEC	C KM/SEC	U KM/SEC
25	295.0	5.322	4.499
30	253.2	5.184	4.470
35	221.8	5.083	4.459
40	197.5	5.005	4.455
50	161.9	4.896	4.454
55	148.5	4.857	4.455
60	137.2	4.823	4.454
65	127.5	4.795	4.454
71	117.5	4.766	4.451
80	105.1	4.731	4.446
86	98.2	4.711	4.440
100	85.3	4.672	4.422
120	71.8	4.627	4.38
150	58.2	4.570	4.29
200	44.6	4.477	4.09
250	36.5	4.379	3.89
300	31.1	4.284	3.74
350	27.2	4.199	3.64

8099

N	THICKNESS KM	ALPHA KM/SEC	BETA KM/SEC	RHO G/CC
1	5.0	1.5200	0.0	1.0300
2	1.0	2.1000	1.0000	2.1000
3	5.0	6.4100	3.7000	2.8400
4	49.0	7.8200	4.6125	3.3400
5	160.0	8.1700	4.3000	3.4425
6	100.0	8.4900	4.6000	3.5265
7	90.0	8.8100	4.8000	3.6040
8	90.0	9.3200	5.1925	3.7650
9	100.0	9.9700	5.4925	4.0100
10	100.0	10.4800	5.7900	4.2300
11	100.0	10.8500	6.0300	4.4100
12	100.0	11.1200	6.2000	4.5450
13	100.0	11.3300	6.3150	4.6400
14	100.0	11.4900	6.4000	4.7100
15	100.0	11.6400	6.4650	4.7700
16	100.0	11.7800	6.5310	4.8275
17	100.0	11.9200	6.5910	4.8825
18	100.0	12.0600	6.6490	4.9400
19	100.0	12.1900	6.7040	5.0000
20	100.0	12.3300	6.7550	5.0550
21	100.0	12.4600	6.8050	5.1050
22	100.0	12.5900	6.8525	5.1575
23	100.0	12.7200	6.8975	5.2075
24	100.0	12.8500	6.9450	5.2650
25	100.0	12.9700	6.9950	5.3150
26	100.0	13.0900	7.0450	5.3650
27	100.0	13.2100	7.0950	5.4150
28	100.0	13.3300	7.1425	5.4650
29	100.0	13.4600	7.1875	5.5150
30	100.0	13.5300	7.2325	5.5625
31	100.0	13.6100	7.2775	5.6075
32	98.0	13.6400	7.3000	5.6550

RAYLEIGH WAVE

N	T SEC	C KM/SEC	U KM/SEC
30	257.9	5.089	3.699
40	208.9	4.732	3.601
50	175.7	4.511	3.618
60	151.4	4.369	3.659
80	118.3	4.205	3.739
100	96.7	4.121	3.804
120	81.6	4.072	3.86
150	65.9	4.038	3.93
200	49.7	4.019	3.99
250	39.8	4.015	4.01
300	33.2	4.015	4.01
350	28.5	4.012	3.97

LOVE WAVE

N	T SEC	C KM/SEC	U KM/SEC
25	298.1	5.262	4.405
30	256.2	5.119	4.373
35	224.8	5.012	4.360
40	200.3	4.932	4.355
50	164.4	4.818	4.357
55	150.9	4.776	4.360
60	139.4	4.742	4.363
70	121.0	4.689	4.369
80	106.9	4.649	4.375
100	86.6	4.596	4.384
120	72.8	4.561	4.39
150	58.7	4.528	4.40
175	50.5	4.509	4.40
200	44.4	4.496	4.40
250	35.7	4.477	4.40
300	29.8	4.465	4.40
350	25.6	4.455	4.40
440	20.4	4.443	4.39

CIT 11A

N	THICKNESS KM	ALPHA KM/SEC	BETA KM/SEC	RHO G/CC
1	5.0	1.5200	0.0	1.0300
2	0.5	2.0000	0.8000	1.9000
3	2.0	4.8000	2.8800	2.5400
4	5.0	6.4100	3.7000	2.9000
5	9.0	8.1000	4.6000	3.3200
6	5.0	8.1200	4.6110	3.3250
7	5.0	8.1200	4.6110	3.3300
8	10.0	8.1200	4.6090	3.3350
9	20.0	8.0100	4.5600	3.3500
10	20.0	7.7600	4.4490	3.3750
11	20.0	7.6000	4.3390	3.3900
12	20.0	7.6800	4.3400	3.4100
13	20.0	7.7770	4.3400	3.4250
14	20.0	7.8500	4.3400	3.4400
15	20.0	8.1900	4.5000	3.4600
16	20.0	8.2100	4.5000	3.4750
17	20.0	8.2100	4.5000	3.4900
18	20.0	8.2100	4.5000	3.5100
19	20.0	8.2100	4.5000	3.5250
20	20.0	8.2100	4.5000	3.5400
21	20.0	8.2100	4.5000	3.5600
22	20.0	8.2100	4.5000	3.5700
23	20.0	8.2100	4.5000	3.5900
24	20.0	8.2400	4.5000	3.6050
25	40.0	8.8000	4.8000	3.6300
26	50.0	9.1500	5.0400	3.6900
27	10.0	9.7600	5.4000	3.7800
28	140.0	9.7800	5.4000	4.0200
29	100.0	9.8000	5.4000	4.2300
30	100.0	11.1200	6.2000	4.4000
31	100.0	11.1800	6.2300	4.5600
32	100.0	11.3500	6.3220	4.6300
33	200.0	11.6000	6.4210	4.7400
34	200.0	11.9200	6.5500	4.8500
35	200.0	12.2000	6.6900	4.9600
36	200.0	12.4000	6.7800	5.0700
37	150.0	12.5500	6.8500	5.1500
38	100.0	12.7000	6.9000	5.2075
39	100.0	12.8500	6.9500	5.2650
40	100.0	13.0000	7.0000	5.3150
41	100.0	13.1000	7.0500	5.3650
42	100.0	13.2000	7.1000	5.4150
43	100.0	13.3000	7.1400	5.4650
44	100.0	13.4200	7.1900	5.5150
45	100.0	13.5700	7.2300	5.5625
46	100.0	13.7000	7.2500	5.6075
47	47.0	13.7000	7.2200	5.6550

RAYLEIGH WAVE

N	T SEC	C KM/SEC	U KM/SEC
25	297.5	5.276	3.812
30	261.3	5.022	3.684
40	211.0	4.683	3.641
50	176.9	4.482	3.697
60	151.8	4.358	3.761
80	117.7	4.224	3.860
100	95.8	4.160	3.901
120	80.6	4.121	3.93
150	65.1	4.083	3.96
200	49.2	4.058	3.97
250	39.5	4.044	3.97
300	33.0	4.035	3.96
350	28.4	4.022	3.92

LOVE WAVE

N	T SEC	C KM/SEC	U KM/SEC
25	298.8	5.249	4.429
30	256.5	5.112	4.405
35	224.8	5.012	4.397
40	200.1	4.936	4.395
50	164.0	4.829	4.400
55	150.4	4.791	4.404
60	138.9	4.759	4.408
70	120.5	4.710	4.416
80	106.3	4.674	4.423
100	86.1	4.625	4.432
120	72.3	4.593	4.44
150	58.3	4.563	4.44
175	50.1	4.545	4.44
200	44.0	4.532	4.44
250	35.4	4.513	4.44
300	29.6	4.500	4.43
350	25.4	4.489	4.42
440	20.3	4.473	4.39

Acknowledgment

We thank Dr. Setumi Miyamura, director of the Dodaira Micro-Earthquake Observatory, for seismograms. Messrs. Masaru Tsujiura, Hideteru Matumoto, and other members of the observatory helped us in the preparation of the data in digital form. We benefited from the discussions with Dr. Seiya Uyeda. Dr. Kazuaki Nakamura kindly read the manuscript and made many valuable suggestions. Miss Tatoko Hirasawa assisted us in the preparation of the manuscript and drawings. We used HITAC 5020 computer system at the computer center of the University of Tokyo.

References

AKI, K., 1960, Study of earthquake mechanism by a method of phase equalization applied to Rayleigh and Love waves, *J. Geophys. Res.*, **65**, 729-740.

AKI, K., 1961, Crustal structure in Japan from the phase velocity of Rayleigh waves, 1, *Bull. Earthq. Res. Inst., Tokyo Univ.*, **39**, 255-283.

ALTERMAN, Z., H. JAROSCH, and C. L. PEKERIS, 1959, Oscillations of the earth, *Proc. Roy. Soc. London, A*, **252**, 80-95.

ALTERMAN, Z., H. JAROSCH, and C. L. PEKERIS, 1961, Propagation of Rayleigh waves in the earth, *Geophys. J.*, **4**, 219-241.

ANDERSON, DON L., 1967, Latest information from seismic observations, Chapter 12, in *The Earth's Mantle*, edited by T. F. GASKELL, pp. 355-420, Academic Press, London.

ANDERSON, DON L., and M, N. TOKSÖZ, 1963, Surface waves on a spherical earth, 1, *J. Geophys. Res.*, **68**, 3483-3500.

BOLT, B., and J. DORMAN, 1961, Phase and Group velocities of Rayleigh waves in a spherical, gravitating earth, *J. Geophys. Res.*, **66**, 2965-2981.

BRUNE, J., and J. DORMAN, 1963, Seismic waves and earth structure in the Canadian shield, *Bull. Seismol. Soc. Am.*, **53**, 167-209.

COOLEY, J. W., and J. W. TUKEY, 1965, An algorithm for the machine calculation of complex Fourier series, *Mathematics of Computation*, **19**, 297-301.

DORMAN, J., M. EWING, and J. OLIVER, 1960, Study of shear-velocity distribution in the upper mantle by mantle Rayleigh waves, *Bull. Seismol. Soc. Am.*, **50**, 87-115.

EWING, M., J. BRUNE, and J. KUO, 1962, Surface-wave studies of the Pacific crust and mantle, in *The Crust of the Pacific Basin*, Geophys. Monograph No. 6, edited by G. A. MACDONALD and H. KUNO, pp. 30-40, American Geophysical Union, Washington, D. C..

FEDOTOV, C. A., and L. B. SLAVINA, 1968, The determination of P velocity in the upper mantle beneath the north-eastern Pacific and Kamchatka (translation of the Russian title), *Izv. Akad. Nauk SSSR, Ser. Geofiz., No.* **2**, 8-31 (in Russian).

HAGIWARA, T., 1958, A note on the theory of the electromagnetic seismograph, *Bull. Earthq. Res. Inst., Tokyo Univ.*, **36**, 139-164.

IIDA, K., 1965, Earthquake magnitude, earthquake fault, and source dimensions, *Journal of Earth Sciences, Nagoya University*, **13**, 115-132.

KANAMORI, H., 1968, Travel times to Japanese stations from Longshot and their geophysical

implications, *Bull. Earthq. Res. Inst., Tokyo Univ.*, **46**, 841-859.

KATSUMATA, M., 1960, The effect of seismic zones upon the transmission of seismic waves, *Kenshin Ziho*, **25** (3), 19-25 (in Japanese).

KOVACH, R. L., 1965, Seismic surface waves: Some observations and recent developments, *Phys. Chem. Earth*, **6**, 251-314.

KOVACH, R. L., and F. PRESS, 1961, Rayleigh wave dispersion and crustal structure in the Eastern Pacific and Indian Oceans, *Geophys. J.*, **4**, 202-216, 1961.

KUO, J., J. BRUNE, and M. MAJOR, 1962, Rayleigh wave dispersion in the Pacific ocean for the period range 20 to 140 seconds, *Bull. Seismol. Soc. Am.*, **52**, 333-357.

MURAUCHI, S., N. DEN, S. ASANO, H. HOTTA, T. YOSHII, T. ASANUMA, K. HAGIWARA, K. ICHIKAWA, T. SATO, W. J. LUDWIG, J. I. EWING, N. T. EDGAR, and R. E. HOUTZ, 1968, Crustal structure of the Philippine Sea, *J. Geophys. Res.*, **73**, 3143-3171.

OLIVER, J. E., M. EWING, and F. PRESS, 1955, Crustal structure and surface-wave dispersion, 4, *Bull. Geol. Soc. Am.*, **66**, 913-946.

OLIVER, J., and B. ISACKS, 1967, Deep earthquake zones, anomalous structures in the upper mantle, and the lithosphere, *J. Geophys. Res.*, **72**, 4259-4275.

PORKKA, M. T., 1966, Surface wave studies on the crust and upper mantle in Eurasia, *Publication No. 90, Institute of Seismology University of Helsinki*, 203-208.

PRESS, F., 1959, Some implications on mantle and crustal structure from *G* waves and Love waves, *J. Geophys. Res.*, **64**, 565-568.

PRESS, F., 1966, Seismological information and advances, in *Advances in Earth Sciences*, edited by P. M. Hurley, pp. 247-286, MIT Press, Cambridge.

PRESS, F., 1968 **a**, The density distribution in the earth, *Science*, **160**, 1218-1221.

PRESS, F., 1968 **b**, Earth models obtained by Monte Carlo inversion, *J. Geophys. Res.*, **73**, 5223-5234.

SAITO, M., and H. TAKEUCHI, 1966, Surface waves across the Pacific, *Bull. Seismol. Soc. Am.*, **56**, 1067-1091.

SANTO, T. A., 1961 **a**, Division of the south-western Pacific area into several regions in each of which Rayleigh waves have the same dispersion characters, *Bull. Earthq. Res. Inst., Tokyo Univ.*, **39**, 603-630.

SANTO, T. A., 1961 **b**, Dispersion of Love waves along various paths of Japan (1), *Bull. Earthq. Res. Inst., Tokyo Univ.*, **39**, 631-651.

SATÔ, Y., M. LANDISMAN, and M. EWING, 1960, Love waves in a heterogeneous, spherical earth, 2, *J. Geophys. Res.*, **65**, 2399-2404.

SUGIMURA, A., 1960, Zonal arrangement of some geophysical and petrological features in Japan and its environs, *J. Fac. Sci., Univ. Tokyo*, Section *2*, **12**, 133-153.

TAKEUCHI, H., J. DORMAN, and M. SAITO, 1964, Partial derivatives of surface wave phase velocity with respect to physical parameter changes within the earth, *J. Geophys. Res.*, **69**, 3429-3441.

TAKEUCHI, H., M. SAITO, and N. KOBAYASHI, 1962, Study of shear velocity distribution in the upper mantle by mantle Rayleigh and Love waves, *J. Geophys. Res.*, **67**, 2831-2839.

TALWANI, M., X. Le Pichon, and M. Ewing, 1965, Crustal structure of the midocean ridges, 2, *J. Geophys. Res.* **70**, 341-352.

TOCHER, D., 1958, Earthquake energy and ground breakage, *Bull. Seismol. Soc. Am.*, **48**, 147-153.

TSUJIURA, M., 1965, A pen-writing long-period seismograph (3), *Bull. Earthq. Res. Inst., Tokyo Univ.*, **43**, 429-440 (in Japanese).

UTSU, T., 1966, Regional differences in absorption of seismic waves in the upper mantle

as inferred from abnormal distributions of seismic intensities, *J. Fac. Sci. Hokkaido Univ. Japan, Ser. VII*, **2**, 359-374.

UTSU, T., 1967, Anomalies in seismic wave velocity and attenuation associated with a deep earthquake zone (1), *J. Fac. Sci. Hokkaido Univ. Japan, Ser. VII*, **3**, 1-25.

VACQUIER, V., S. UYEDA, M. YASUI, J. SCLATER, C. CORRY, and T. WATANABE, 1966, Studies of the thermal state of the earth, 19, *Bull. Earthq. Res. Inst., Tokyo Univ.*, **44**, 1519-1535.

---

50. 長周期表面波による Island Arc 構造の研究

地震研究所 金森博雄 阿部勝征

堂平微小地震観測所の3成分長周期地震計を用い，島弧の深部構造を明らかにするため，周期20から110秒までの Rayleigh 波と Love 波の群速度を測定した．Rayleigh 波と Love 波を分離するために水平成分を波の伝幡方向とそれに直角な方向に分解した．群速度は band-pass filter と group delay time $d\phi/d\omega$ (ϕ: 位相, ω: 角周波数) の両方を用いてきめた．Love 波の群速度は周期 100 秒のところで Banda Sea, West Caroline 島の地震については Aleutian の地震についての値とくらべて約 0.2 km/sec おそい．Rayleigh 波についても同じ傾向がみられた．群速度の差は周期 80 sec で約 0.15 km/sec である．Banda Sea, West Caroline 島からの伝幡径路は大部分深発地震発生面の大陸側にあり，Aleutian からのものは海側にある．このことは深発地震発生面をさかいとして大陸側ではマントル内の速度がおそく，海側では速いことを意味する．いくつかのモデルについて分散曲線を計算した結果，Rayleigh 波，Love 波両者の観測結果を同時に説明しうるモデルが得られた．このモデルでは深発地震帯の大陸側のマントルでは海側のマントルにくらべて深さ 30 から 60 km にわたって S 波の速さが約 0.3 から 0.4 km/sec 程度遅い．大陸側からきた波の分散曲線はユーラシア大陸の平均的分散曲線と大体一致する．
